

The Effects of Aspect Ratio in Magnetic Field Structure around the outermostsurfaces of L=1 Helical Systems

M. Aizawa, Y. Nakata and Y. Nagamine

Institute of Quantum Science, College of Science and Technology,

Nihon University, Tokyo, 101-8308, JAPAN

E-mail:aizawa@phys.cst.nihon-u.ac.jp

Abstract

The L=1 torsatron systems having a spatial magnetic axis have been studied. The features of magnetic field properties between high and low helical coil aspect ratio systems have been examined. And magnetic field structures around the outermostsurfaces of several systems which are different pitch modulation α^* and coil aspect ratio, have been studied by examining the Lyapunov characteristic exponents. As the result, desirable properties of magnetic field of low aspect coil systems with negative α^* have been confirmed.

1. Introduction

If we consider a compact system, a small field period number of the helical magnetic field N and low coil aspect ratio system is desirable for nuclear fusion device construction. The trapped particle confinement in the L=1 helical system with a large N is considerable satisfactory by particle orbits tracing and calculating the neoclassical transport particle and heat fluxes [1]. On the contrary, particles transport properties of compact system become worse due to large usual toroidal effects. We have improved particles transport by controlling the effective curvature toroidal term defined as the sum of usual toroidal curvature term and one of the nearest satellite harmonics of helical field term [1]. The improvement of particles confinements evaluated by the Boozer coordinate is observed. But their effects are more limited than that of large aspect ratio cases [2]. The transport properties of these compact systems are worse than large aspect ratio devices. And the

structures of magnetic field are also studied from viewpoint of the effective curvature term.

2. Different coil aspect ratio devices

We have examined several type devices with different coil aspect ratio $A_C \equiv R_0 / a$. A minor radius a is hold constant ($= 0.3[m]$) and a helical coil current is 1000[kA] in each case. The length of one helical field period is also fixed with standard case $N_0 = 17$ device so that new coil aspect ratio will be obtained for an appropriate N by $A_C = N A_{C0} / N_0$. The subscript “0” denotes standard device case. The characteristic parameters are summarized in the reference [3].

3. Lyapunov characteristic exponent

The Lyapunov characteristic exponent (LCE) gives the rate of exponential divergence from perturbed initial conditions. The equations of a magnetic field line have three LCEs, and the positive maximum LCE λ_l decides a chaotic property of system. Let the base solution as $\tilde{X}(\ell)$, where ℓ is the arc length of field line, and perturbed solution as $\hat{X}(\ell)$. The deviation vector $w(\ell) = \hat{X}(\ell) - \tilde{X}(\ell)$ and its magnitude $\varepsilon(\ell) = |w(\ell)|$ are introduced to calculate λ_l , where λ_l is defined by

$$\lambda_l = \lim_{L \rightarrow \infty, \varepsilon(0) \rightarrow 0} \lambda_l^{(L)}, \quad \lambda_l^{(L)} = \frac{1}{L} \log \frac{\varepsilon(L)}{\varepsilon(0)}. \quad (1)$$

It is difficult to calculate λ_l by using eq. (1) directly. Because the finite digits of computer treatment cannot process wide range data defined by eq. (1). Though the field line equations are non-linear equation, the equations satisfied for small deviation vector are linear equation. By using this property, it can be possible to calculate λ_l for small interval $\Delta\ell$ to suppress wide range calculation. The starting deviation vector $w_{st}(n\Delta\ell)$ which is rescaling vector along $w(n\Delta\ell)$ is introduced and is followed until $(n+1)\Delta\ell$, then this vector is defined as the ending deviation vector $w_{en}((n+1)\Delta\ell)$ [4]. Eq. (1) is modified and becomes suitable for numerical calculation as

$$\lambda_l^{(L)} = \frac{1}{L} \log \left(\frac{|w_{en}(\Delta\ell)|}{\varepsilon(0)} \times \frac{|w_{en}(2\Delta\ell)|}{\varepsilon(0)} \times \cdots \times \frac{|w_{en}(L = n\Delta\ell)|}{\varepsilon(0)} \right). \quad (2)$$

The practice program is coded and checked by testing of well-known Lorentz model equations.

4. Magnetic Field Properties

Here after, the value of λ_l is evaluated by setting $L=1000$ in eq. (2). Fig.1 shows the $\lambda_l^{(L)}$ against L which is the arc length of field line. The four different period numbers $N=5$ (Fig.1(a)), $N=8$ (Fig.1(b)), $N=12$ (Fig.1(c)) and $N=17$ (Fig.1.(d)) cases are shown, and the each system has no pitch modulation. The r_0 is starting point of field line.

In Fig2, the maximum Lyapunov exponents $\lambda_l^{(L)}$ at $L=1000$ are shown against system period number N in the three cases $\alpha^*=-0.2$ (Fig.2(a)), $\alpha^*=0.0$ (Fig.2(b)) and $\alpha^*=0.2$ (Fig.2(c)). In Fig.3, the average values of maximum Lyapunov exponents $\lambda_l^{(L)}$ at $L=1000$ are shown against pitch modulation parameter α^* in four different period number N cases.

5. Conclusion

We have confirmed that the parameter α^* controls the chaotic properties of fields around the outermost surface in large N , namely large A_c systems. On the other hand, low N system has low λ_l properties though α^* dependency is weaker than high A_c cases. It takes much calculation time for λ_l in our helical system where we evaluate field from coil current directly. The reductions of execution time are our task that we must resolve.

References

- [1] M. Aizawa and S. Shiina; *Phys. Rev. Lett.* Vol. 84, 2638 (2000)
- [2] M. Aizawa and Y. Nagamine; *ECA* Vol. **35G** P-1.111 (2011)
- [3] M. Aizawa and Y. Nagamine; *ECA* Vol. **37D** P-4.148 (2013)
- [4] E.Ott; “*Chaos in Dynamical Systems, 2nd ed.*” Cambridge University Press (2002)

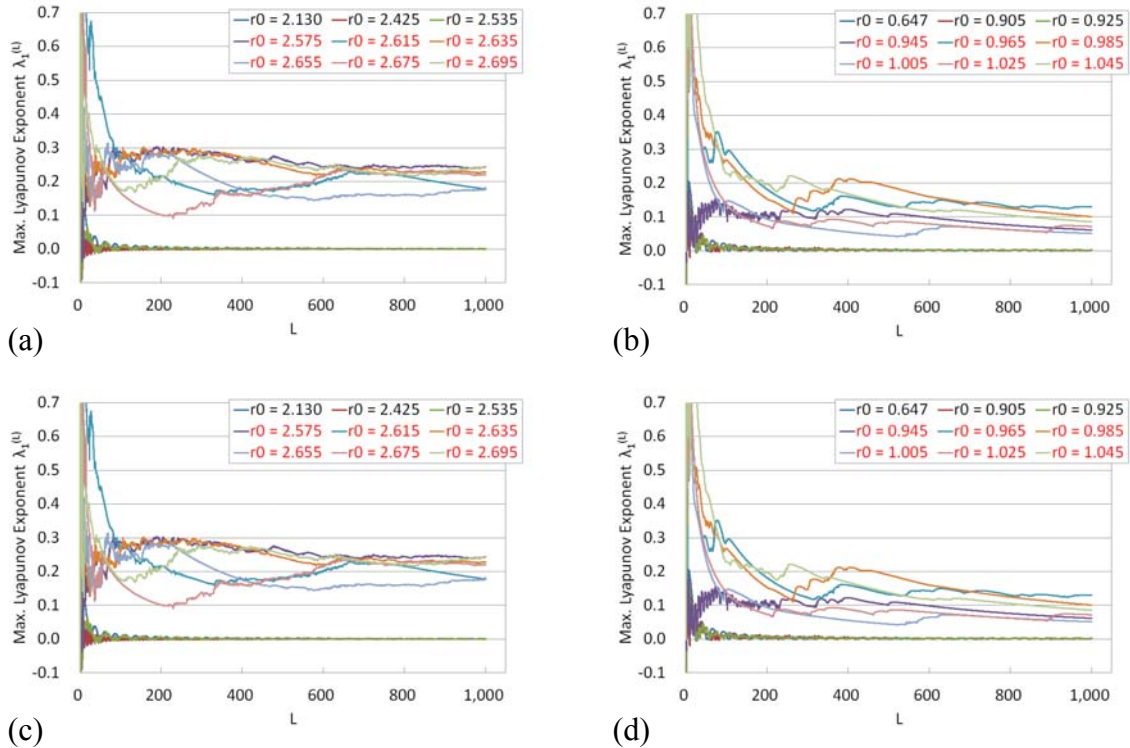


Fig.1 The maximum Lyapunov exponents $\lambda_1^{(L)}$ are shown against L which is the arc length along a field line. The four different period numbers $N=5$ (a), $N=8$ (b), $N=12$ (c) and $N=17$ (d) cases are shown, and the each system has no pitch modulation, that is, $\alpha^*=0.0$.

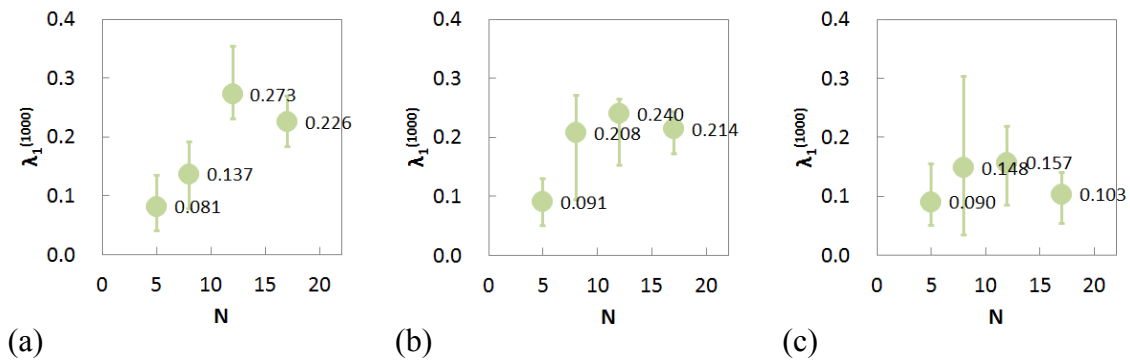


Fig.2 The maximum Lyapunov exponents $\lambda_1^{(L)}$ at $L=1000$ are shown against system period number N in the three cases $\alpha^*=-0.2$ (a), $\alpha^*=0.0$ (b) and $\alpha^*=0.2$ (c).

Fig.3 The average values of maximum Lyapunov exponents $\lambda_1^{(L)}$ at $L=1000$ are shown against pitch modulation parameter α^* in four different period number N cases.

